

3D Non-destructive Micro-structure Characterization of Aramid and Steel Fibre-Reinforced Concrete using X-ray Computed Tomography

Savas Erdem (Corresponding author)
School of Civil Engineering, Istanbul University
34420, Avcilar, Istanbul, Turkey, E-mail: savas.erdem@istanbul.edu.tr

Ezgi Gurbuz
School of Civil Engineering, Istanbul University
34420, Avcilar, Istanbul, Turkey,

Abstract

A non-destructive X-ray computed tomography technique was utilized to investigate 3D microstructure (voids, fibres and cracks) of the composite materials subjected to impact loading. A total of three different types of concrete mixes with and without fibres of steel and aramid fibres were cast and investigated. In general, the results indicate that all specimens experienced a significant increase in air voids after being subjected to the high rates of loading but the aramid and steel mixes experienced less and small cracks. In addition, the fibre distribution was less homogeneous throughout the specimen in the case of the aramid fibre composite.

Keywords: Concrete; Non-destructive analysis; 3D microstructure; X-ray computed tomography.

1. Introduction

Understanding the structure-properties relationships and deformation and failure mechanism at different length scales is fundamental to achieving a more advanced understanding of how to apply and optimize concrete materials [1]. X-ray CT is a completely non-destructive technology and provides a rapid means of gathering the 3D data from a contiguous series of 2D measurements that are needed for such analyses. X-ray CT systems are used to generate a map representing the density at every point in the microstructure. Using an X-ray CT system along with digital image analysis techniques allows cracks, aggregates, air voids (distribution, shape, average size, orientation etc.) to be visualized and evaluated, and thus the method can be used to study the structure/property relationships in composites.

The fibres used in the literature are prominently steel fibres. The addition of steel fibres to structural materials improves the impact resistance, the compression toughness, flexural strength and as well as deformation capability [2-4]. In addition to steel fibres, aramid fibres are a new class of material becoming more and more popular for the reinforcement of civil engineering materials. This type of fibre is mainly used for components that are subjected to impact or other dynamic loading to prevent sudden and catastrophic failure [5].

In this study, a nondestructive X-ray computed tomography technique was utilized to investigate 3D microstructure (voids and cracks) of the three different types of composite mixes with and without fibres of steel and aramid fibres subjected to high-rates of loading.

2. Experimental program

In all, a total of three different types of concrete mixes with and without fibres of steel and aramid fibres were cast and investigated. For all mixtures, the volume fraction of cement, sand, coarse aggregate, fibres and free water were kept constant. The only difference between the mixtures was the type of fibres. The volume fractions of fibres in concrete were 1.0 %. The mix proportions are shown in Table 1.

Table 1. Concrete mix properties

	Cement (kg/m ³)	Coarse aggregate (kg/m ³)	Fine aggregate (kg/m ³)	Water (kg/m ³)	Fiber (kg/m ³)
Normal Composite	450	985	865	205	-
Steel Fiber Composite	450	985	865	205	78
Aramid Fiber Composite	450	985	865	205	9.8

Impact test were carried out using a Rosand type 5 instrumented falling weight impact tester. 150 mm diameter and 50 mm height cylinder specimens were used for the impact testing and the hammer was dropped from 500 mm height. An X-ray CT system (Venlo H-350/225) with IMPS operating software was used for scanning the specimens. The 350kV mini focus source, which has the necessary power to penetrate the concrete mix specimens with a reasonable resolution was used to obtain the 2D images. The specimens were fixed on the turn table to ensure that it does not move while the X-ray is scanning. The captured images from the X-ray CT system after impact loading were then analyzed and converted to 2D images using the standard capabilities of an image analysis software package (Image J).

3. Results and discussion

Figure 1 (a) shows the air voids distribution within a concrete cube after being tested under the impact loading. The 3D view of the specimen is constructed as shown in Figure 1 (b). From the air void fractions calculated throughout the specimen's height, more damage can be observed at the top of the specimen (between 70 and 100 mm) with higher air voids fraction compared to the other sections. This is probably due to the direct contact of the surface to the impact load which is applied on the top of the cube that has caused the cube to break into pieces and loss of fine material. In addition, this is proved by the cracks observed on the X-ray slices within the top section, where these cracks propagated and coalesced through the specimen's height, down to the bottom section. The images of the cracks at different heights which represent the different sections are shown in Figure 2.

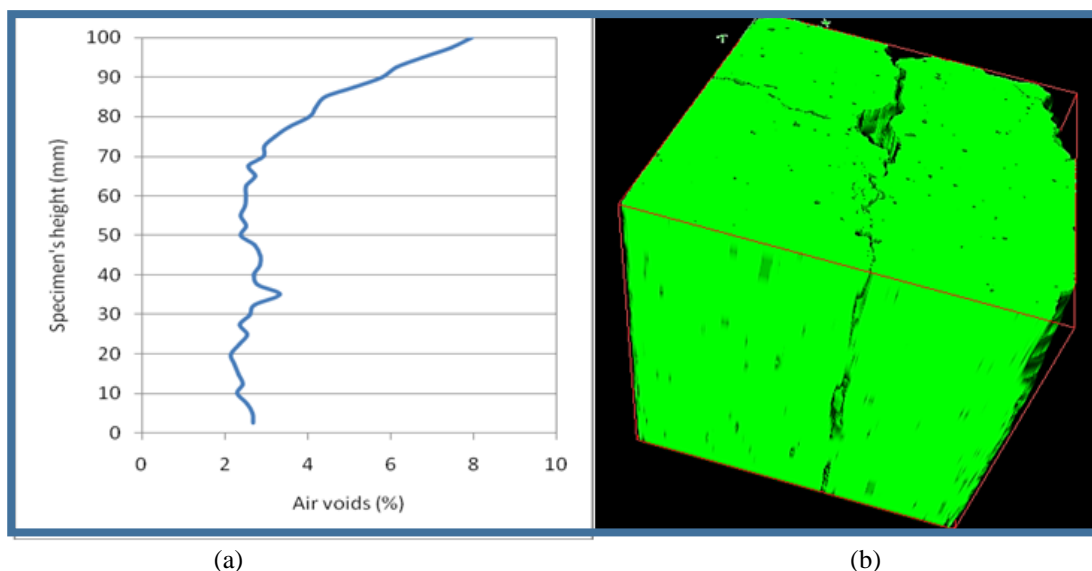


Figure 1: Air Voids Distribution (a) and 3D View (b) of Normal Composites

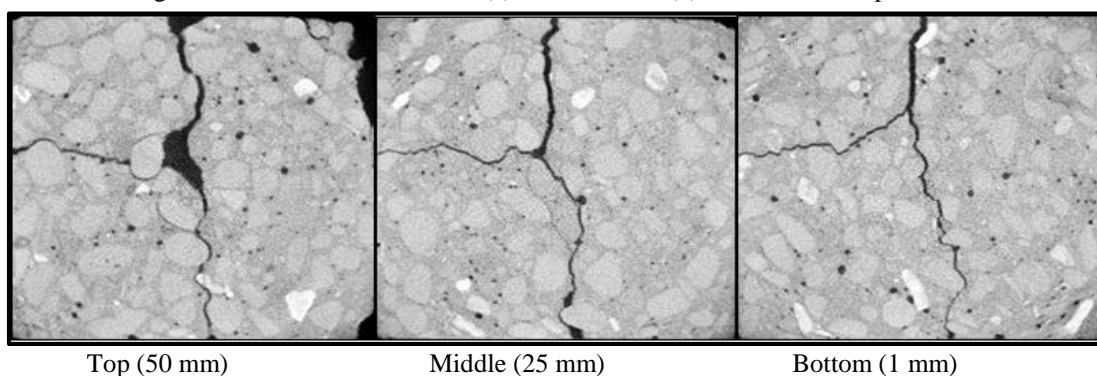


Figure 2. The Images of The Cracks at Different Heights

For the concrete specimen added with steel fibre, the air voids and steel fibre distributions within the specimen are presented in Figure 3. The steel fibres act as reinforcement within the concrete specimen and prevent the concrete from filling up the spaces during compaction.

From the analysis (Figure 3), it shows that the aramid fibres settle to the bottom after the compaction or in other words the aramid fibre distribution is not homogeneous throughout the specimen. Whereas, the air voids were found higher at the height of 5 mm close to both edges of the specimen (top and bottom sections). The 3D views of the specimen are constructed as shown in Figure 4 (a)-(b). Based on Figure 5 (a), it can be seen that the increase in the air void content at the top section is not mainly contributed by the cracks but also the loss of fine particles as a result of the impact load. On the other hand, high air void content observed at the bottom section is also contributed by the existing void particularly within the circumference area. The crack formation and propagation seems consistent from the initial point of hitting towards the bottom section. This could possibly provide much larger distances between the cracks (holding energy) and displace the site at which shock-wave induced stress exceeds a critical value and cracks begin. However larger crack opening within the top section can be observed from the CT images (as shown by the darker crack area – Figure 5 (a)) compared to the crack within the middle and bottom sections. In other words, the larger the crack opening, the darker the crack area detected within the CT images. As is noticed, the higher AV between 35 and 50 mm is contributed by a single large AV particle that forms at the middle of the specimen (Figure 5 (b)). This is due to the fact that the specimen with steel fibre needs more compaction effort as the steel fibres form sort of reinforcement within the specimen which could prevent the ‘flow of the concrete or cement paste to fill up the spaces’ (within the mould)). It should be also mentioned that specimen scanned with D=150 will come out with beam hardening (Figure 5 (b)) problem which is due to improper energy or wave travel from edge to edge and the fibre distribution is not homogeneous at that part of the specimen (Figure 5 (c)).

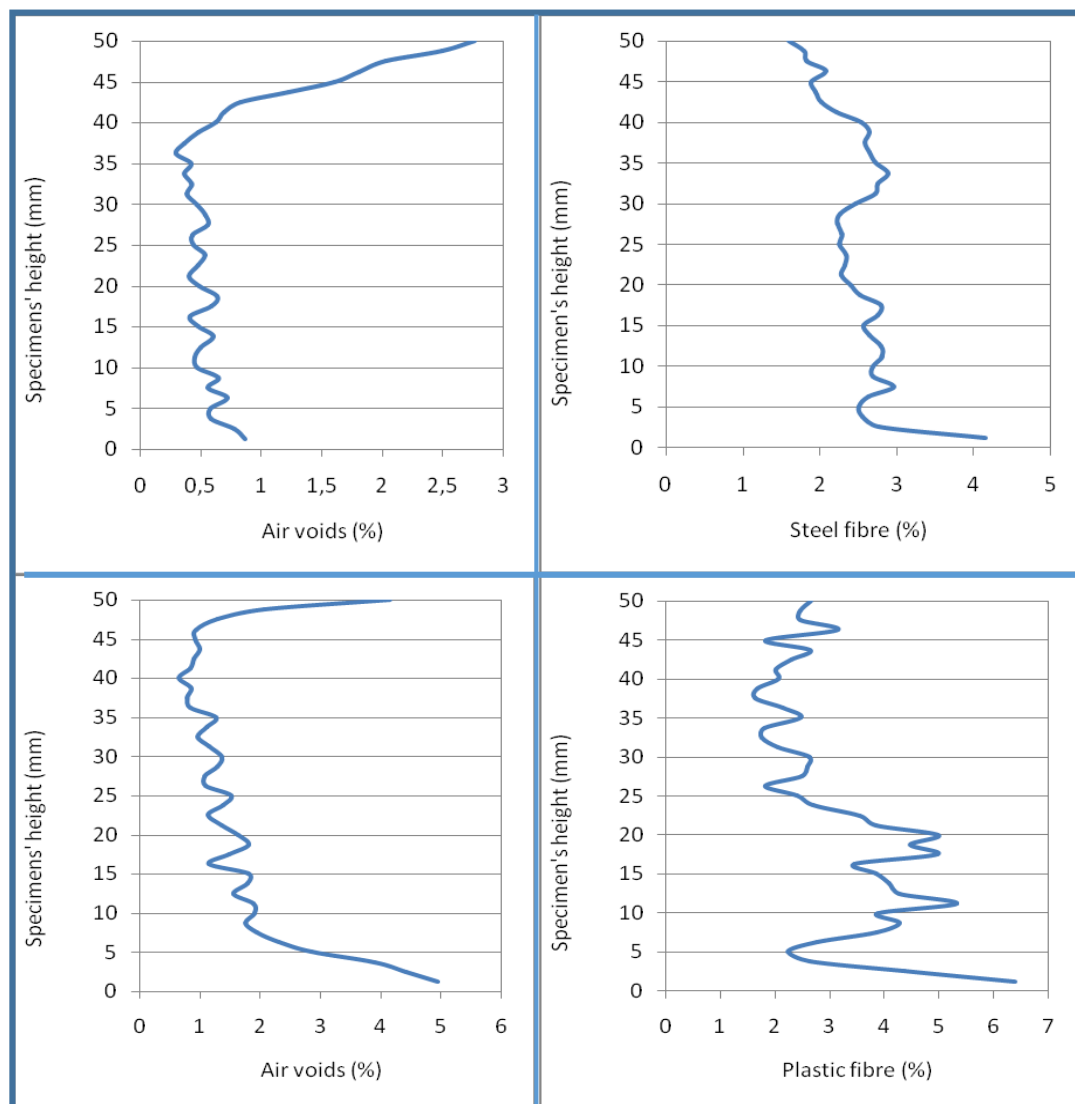
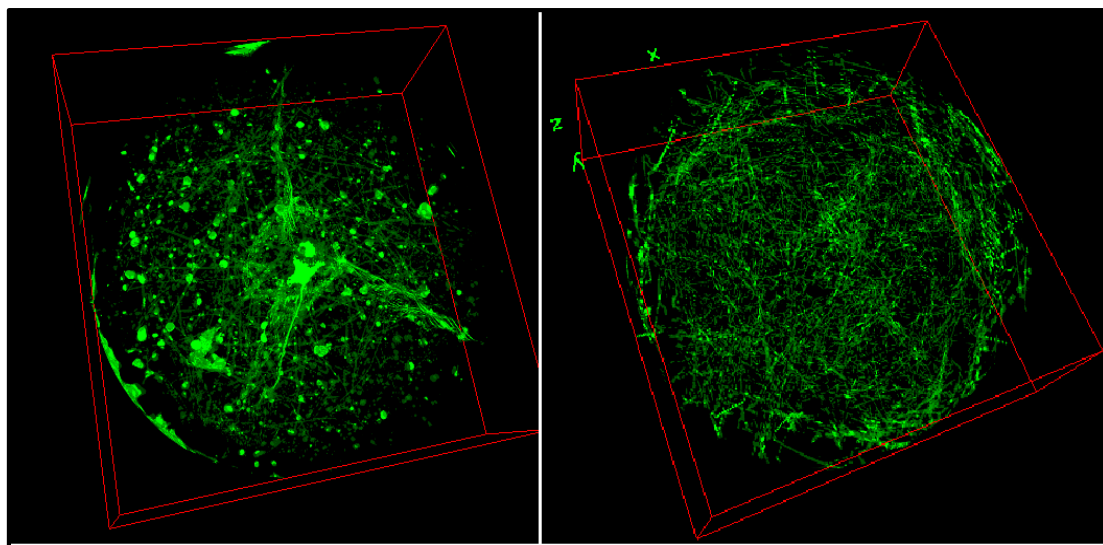
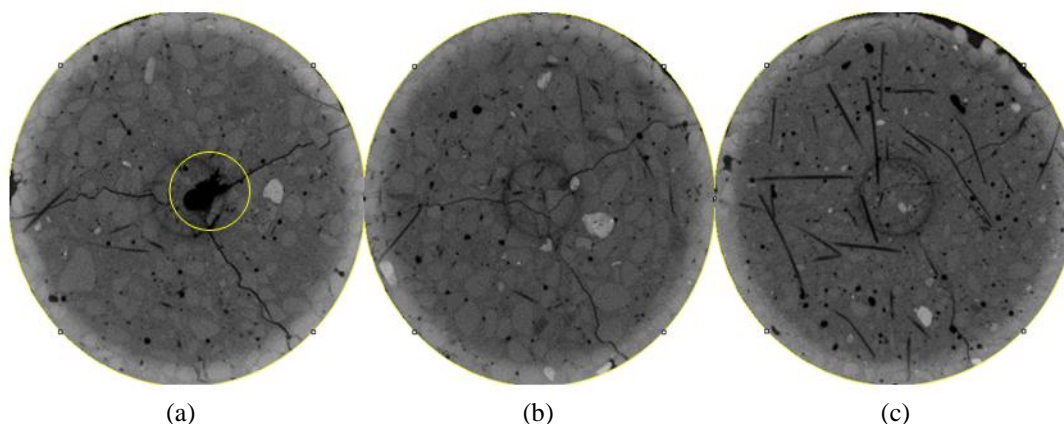


Figure 3: Air voids and steel/plastic aramid fiber distributions within the specimen



(a) (b)
Figure 4: 3D view of the plastic aramid fiber and voids formation (a) and steel fiber (b) within the specimen



(a) (b) (c)
Figure 5: Crack images of the aramid composite at different heights and the beam hardening in the steel composite

4. Conclusions

In the light of the findings obtained from this experimental study, the following conclusions can be drawn:

- The analysis in air void distribution is demonstrated to provide a good basis on which to evaluate the deterioration of concrete subjected to impact loading.
- The high rates of loading would tend to form a network of inter-connected cracks between the pores and existing micro-cracks.
- Micro-crack characteristics are governed by significantly different mechanisms in normal and fiber-reinforced composites under impact. The more ductile behaviour of fiber-reinforced composites led to less number and smaller cracks in the matrix at micro-scale.
- The micro-structural data obtained could be used to develop a multi-scale finite element model to simulate and predict the behaviour and fracture damage of composites subjected to high-rates of loading.

References

- [1] Allison, P. G., Moser, R. D., Schirer, J. P., Martens, R. L., Jordon, J. B., & Chandler, M. Q. (2014). In-situ nanomechanical studies of deformation and damage mechanisms in nanocomposites monitored using scanning electron microscopy. *Mater Lett*, 131, 313-316.
- [2] Marar, K., Eren, O., & Celik, T. (2001). Relationship between impact energy and compression toughness energy of high-strength fibre-reinforced concrete. *Mater Lett*, 47, 297-304.
- [3] Aruntas, H. Y., Cemalgil, S., Simsek, O., Durmus, G., & Erdal, M. (2008). Effects of super plasticizer and curing conditions on properties of concrete with and without fibre. *Mater Lett*, 62, 3441-3443.
- [4] Rambo, D. A. S., Silva, F. A., & Filho, R. D. T. (2014). Mechanical behaviour of hybrid steel-fibre self-consolidating concrete: Materials and structural aspects. *Mater Des*, 54, 32-42.
- [5] Subramani, T., Kuruvilla, R., & Jayalakshmi, J. (2014). Nonlinear analysis of reinforced concrete column with fibre reinforced polymer bars. *Int J Eng Res App*, 4, 306-316.